

LIGHT LITHOPHILE ELEMENT TRENDS IN NAKHLITE NWA 817 PYROXENES: IMPLICATIONS FOR WATER ON MARS. D. S. Musselwhite¹, A.H.Treiman¹, and C. Shearer² ¹Lunar and Planetary Institute (3700 Bay Area Blvd., Houston, TX 77058, musselwhite@lpi.usra.edu, treiman@lpi.usra.edu), ²Institute for Meteoritics (Univ. of New Mexico, Albuquerque, NM 87131, cshearer@unm.edu)

Abundances of LLE (Li, B, Be) are strongly zoned in augite grains of the NWA 817 nakhlite [1,2]. Be and B consistently increase to grain rims (like Fe* and Ti), consistent with their geochemical behavior as incompatible elements. Li abundances increase outward in some rims, but decrease significantly in others. The cause of this bipolar behavior is not clear. LLE are not zoned in augites in the nakhlites Nakhla and Lafayette [3], which may suggest LLE mobility in late- and post-igneous cooling [4].

Introduction: The light lithophile elements (LLE), Li, B, and Be, can be useful as tracers of water-rock processes. They are analyzed together and behave nearly identically in igneous fractionation [4], but Li and B are soluble in aqueous solutions while Be is not [5,6]. Differences in the behavior of Be versus Li and B in pyroxenes of the shergottite Martian meteorites has suggested that the meteorites' parent magmas lost significant quantities of water along with Li and B [3]. However, similar LLE behavior is also reported in lunar basalts and shocked Earth basalts [7]. LLE in pyroxenes of the nakhlite martian meteorites (Nakhla and Lafayette) behaved identically, but not in a manner consistent with igneous fractionations [3,4].

To help resolve these issues, we investigated LLE abundances in augite phenocrysts of the NWA817 nakhlite [1,2]. It was chosen because it cooled very rapidly; its LLE abundance patterns should reflect igneous processes only.

Analytical Procedures: All measurements were made on a single thin section (554). Major and minor element profiles were measured using the Cameca sx100 electron microprobe at NASA/JSC, using a focused beam at 15kV and 20 nA. Peak counting time was 20 seconds on each point. These profiles were then examined for suitable rim/core targets for SIMS analysis. Eleven major and minor element profiles were measured. Of these, 7 (#'s 1-6 and 10) were analyzed for Li, Be, B, Ti, Ca using the Cameca ims 4f ion probe at the Univ. of New Mexico, Institute for Meteoritics. Before analyses, the thin section was washed in a 1% manitol solution and rinsed in ultra pure water to eliminate B contamination [8], then gold coated. Prior to each analysis, the sample surface was cleaned using a rastered ion beam and imaged to better define the location of the analysis. Analysis was conducted with a 10 kV, 10 nA O⁺ beam with a spot diameter of 10 to 15 μ m. All mass peaks (^{18.7}background, ⁴⁴Ca⁺, ⁴⁸Ti⁺,

⁷Li⁺, ⁹Be⁺, ¹¹B⁺) were counted for 2 seconds except ³⁰Si⁺ which was counted for 4 seconds. Each spot was analyzed for ten count cycles. Internal precision (counting statistics) was better than 1% for all trace elements. The LLE calibration curves ($[(\text{element}^+ / ^{30}\text{Si}^+) * \text{SiO}_2\%]$ versus element abundance) had correlation coefficients greater than 0.997.

Results: Major element (Mg, Fe, Ca) zoning patterns are similar in all clinopyroxene profiles. Cores are generally homogeneous in Mg, Fe and Ca. Minor element abundances are also relatively constant, although in some core profiles showed variations of up to 20. The cores show some spikes in Al abundance, some of which correspond to spikes in abundances of other elements.

Augite grains show two types of rim profiles: sharp and "plateau". Figure 1 shows an augite grain, with both types of rim: the left is sharp; the right is a more gradual rim with a hump or plateau.

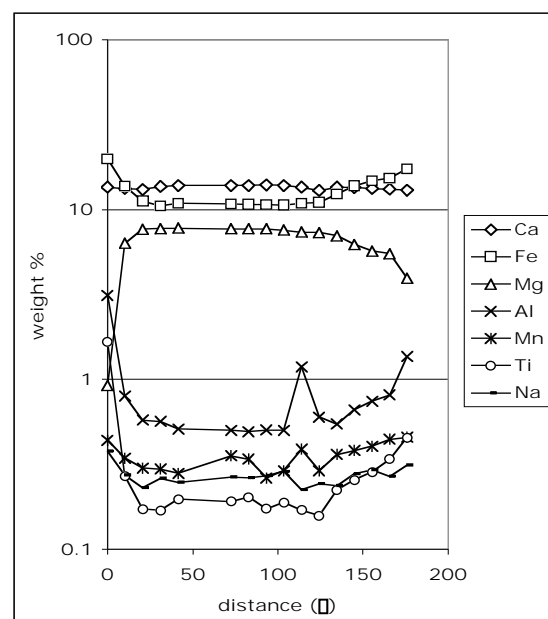


Figure 1: Major and minor element profile of NWA817 pyroxene, profile 10. Data from electron microprobe.

The sharp-type rims display a monotonic variation in element concentration from core to rim. Rims vary in width from 20 to 40 μ m depending on crystallographic orientation. These rims have been described by [2] and major and minor elemental patterns described here are consistent with their observations. The sharp rims are seen only adjacent

to the mesostasis. This sharp zonation pattern is interpreted as a primary magmatic growth rim.

The “plateau”-type of rim, not reported previously, displays a more gradual change or plateau in concentration followed by a sharper change closer to the rim (right side, Fig.1). Plateau-type rims are approximately 50 μ m wide and occur adjacent to mesostasis. Since the major and minor element trends are broadly the same from core to rim in both rim types, there is the possibility that the plateau pattern is merely an artifact of a difference in crystallographic orientation. However, the flattening of the trend is distinct from the monotonic change in the values seen in the sharp rims. Some of the sharp rims are up to 40 μ m wide and do not display this flattening of the elemental trends away from the rim. In addition (and perhaps more convincingly) there is a difference in Li patterns between the two rim types as discussed below.

LLE profiles for the grain of Figure 1 are shown in Figure 2, and are typical of the other analyzed grains. Zoning patterns for B and Be are similar in the two rim types. Be concentrations consistently rise from 0.02 to 0.06 ppm in the core to 0.2 to 0.7 in the rim. B concentrations rise from ~1 ppm in the core to as high as 12 ppm in the rim in the sharp-type rims and up to 4 ppm in the plateau type.

However, Li behaves differently in the two rim types. For all grains studied, Li decreases across sharp rims from ~6 ppm in the cores to as low as 2 ppm in the rim. In the plateau-type rims, Li rises slightly (but significantly) above the core value.

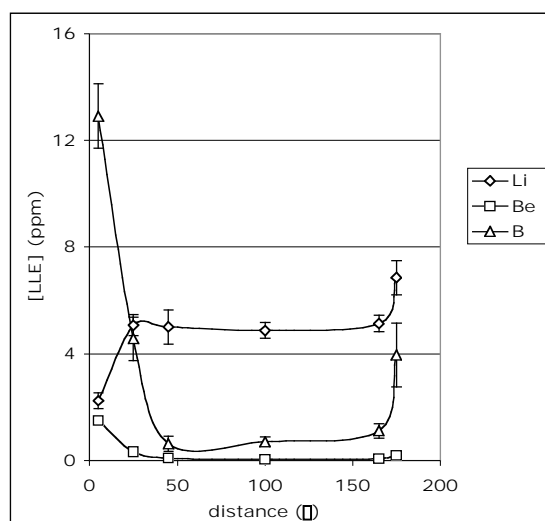


Figure 2: LLE profile of NWA817 pyroxene, line 10. Data from SIMS.

Discussion: The fact that the concentrations of major, minor and light lithophile elements are constant through out much of the core is evidence for

their growth within a large magma reservoir. The sharp changes observed for elemental concentrations in the rims likely occurred during or following accumulation of the pyroxenes.

The consistent rise in B and Be in the pyroxene rims is typical of incompatible element behavior – elemental concentration rises in the melt as crystallization proceeds causing the concentration in the later crystallizing or outer portion of the crystal to increase. Likewise, the increase in Li in the plateau-type rims is understandable as typical incompatible element behavior during late stage crystallization. However, the Li results in the sharp-type rims are puzzling in this regard. Localized depletion of Li in the intercumulus liquid adjacent to the mesostasis-side of the late crystallizing pyroxene is one possible explanation. Perhaps Li is taken up by some late crystallizing minor phase. Li is known to form spinel-structure minerals under special circumstances [9]. So, it is possible that Li is taken up by late crystallizing oxide grains. Identification of suitable (i.e., large) oxide grains for SIMS analysis of LLEs would be a good test of this idea. The differences between the two rim types could represent different non-equilibrium crystallization paths in different pockets of mesostasis. For example, some mesostasis pockets in Nakhla have pigeonite while others have augite [10]. Furthermore, plagioclase could have crystallized (or not) at any point in the evolution of a particular mesostasis pocket.

The observation that B concentration rises in the sharp-type rims even though Li falls is, inconsistent with H₂O loss during late crystallization as both elements are highly soluble in H₂O-rich fluids [5]. Lenz *et al.* [3] proposed outgassing of water during crystallization of the shergottites Shergotty and Zagami to explain the decrease in Li and B in the late forming pyroxene rims. In contrast, they noted an increase in these elements in the rims for the naxhlites, Nakhla and Lafayette as we have found in the “plateau-type” rims in NWA 817 but in contrast to our results for the sharp-type rims.

References: [1] Grossman, J.N. and Zipfel, J. (2001) *MAPS* **36**, A300 [2] Sauter *et al* (2002) *EPSL* **195**, 223-238. [3] Lentz, R.C.F. *et al.* (2001) *GCA* **65**, 4551-4565. [4] Herd *et al.* (2004) *Amer. Mineral.* **89**, 832-840. [5] Brenan, J.N. *et al* (1998) *GCA* **62**, pp 3337-3347. [6] Ryan, J.G. and Langmuir, C.H. (1993) *GCA* **57**, 1489-1498. [7] Chaklader *et al.* (2004) *PLPS XXXV*, #1397. [8] Hervig, R.L. *et al.* (2002) *Am. Min.* **87**, 1015-1024. [9] Kawai, H. *et al.* (1998) *J Mater Chem* **8** 1273 [10] Harvey, R.P. and McSween, H.Y. (1992) *GCA* **56**, 1655-1663.